Green Analytical Chemistry 13 (2025) 100283

Contents lists available at ScienceDirect

Green Analytical Chemistry

journal homepage: www.elsevier.com/locate/greeac

Composite microbeads of cellulose acetate upcycled from waste for water remediation

Lorenzo Antonelli [a], Susanna Grasso [a], Massimo Giuseppe De Cesaris [a], Nina Felli [a], Chiara Dal Bosco [a], Stefano Cinti [b,*], Alessandra Gentili [a,*]

[a] Department of Chemistry, Sapienza University, P.le Aldo Moro 5, Rome 00185, Italy
[b] Department of Pharmacy, University of Naples Federico II, Naples, Italy

ARTICLE INFO

Keywords:
Plastic waste
Recycling
Green chemistry
Composite sorbents
Water remediation
Breakthrough curves

ABSTRACT

The rising level of contaminants in the environment highlights the urgent need for the development of effective sorbents that can be applied to remediate contaminated water. Additionally, if sorbents can be prepared by recycling waste, this is a further added value. This study has aimed to develop a sustainable nanocomposite sorbent of cellulose acetate (CA), a bioplastic that can be recycled from different types of waste, including filters from cigarette butts. After an efficient cleaning protocol, the recovered CA was used to prepare microspheres via an emulsion precipitation technique, in combination with activated carbon as adsorption filler (20 % w/w). The sorption performance of this material was evaluated in flow-through systems, i.e. glass cartridges packed with the microspheres, by simulating a filter for water remediation at the laboratory scale. An experimental 2^3 factorial design was performed to define the best operational conditions of the instrumental setup, defining the flow rate, amount and chemical nature of the packed microbeads. The adsorption performance was tested towards 40 common contaminants chosen as model compounds. To investigate the retention behaviour of the individual analytes, the Gompertz mathematical model was chosen, as it is useful for fitting the sigmoidal release pattern of contaminants from the packed cartridge. Competitive removal studies revealed differential retention based on analyte polarity, with retention capacities spanning from 2.2 – 4.2 μg of each contaminant per gram of sorbent, with a total loading capacity on the order of 125 $\mu g/g_{sorbent}$. The adsorption studies demonstrated the composite potential for water remediation operations, coupled with advantages in terms of recyclability and sustainability of the material.

1. Introduction

Although 71 % of the Earth's surface is covered by water, only 1 % is freshwater suitable for human consumption [1,2]. The problem of water scarcity is further compounded by pollution caused by anthropic activities, such as the use of fertilizers and pesticides in agriculture, veterinary drugs in livestock farming, and other contaminants from the industrial sector [3]. This pollution has significant consequences not only for the ecosystems, but also for human health as exposure to contaminated water can cause a range of illnesses.

In response to these problems, the scientific community is working hard to develop solutions for water purification to remove physical, chemical, and biological contaminants. Among the most used purification techniques there are oxidation, phytoremediation, bioremediation, membrane filtration, adsorption, reverse osmosis, ion exchange, electrodialysis, etc. These techniques differ in terms of treatment time, costs, industrial scalability, and release of secondary chemical residues [4]. Among them, adsorption stands out for its low cost (5–200 USD for m^3 of treated water against 10–450 USD of other techniques), efficiency (up to 99.9 % mainly depending on the sorbent nature), versatility, and ease of operation.

Sorbent materials like activated carbon, zeolites, silica, and (bio) polymer-based materials are widely used due to their high surface area and porosity, which allows them to trap pollutants effectively [5]. These materials must be non-toxic, readily available, and ideally derived from natural or waste sources to minimize their environmental impact [6,7]. Additionally, they should be easy to dispose of at the end of their life-cycle [8]. Among them, activated carbon is an excellent sorbent, particularly of nonpolar and medium-polar substances, due to its imperfect graphite-like structure, the presence of heteroatoms, and its

* Corresponding authors.
E-mail addresses: stefano.cinti@unina.it (S. Cinti), alessandra.gentili@uniroma1.it (A. Gentili).

https://doi.org/10.1016/j.greeac.2025.100283
Received 10 March 2025; Received in revised form 15 May 2025; Accepted 24 May 2025
Available online 25 May 2025
2772-5774/© 2025 The Authors. Published by Elsevier B.V. This is an open access article under the CC BY license (http://creativecommons.org/licenses/by/4.0/).

high surface area, often greater than 1000 m^2/g [9,10]. This material can be obtained from natural or waste sources, such as fruit peels and nutshells [11,12]. For example, a study by Bansode et al. demonstrated that activated carbons, made from almond and pecan shells, were effective at removing volatile organic compounds from water, performing similarly to conventional activated carbons derived from fossil fuels [13]. Plastic waste can also be repurposed to produce activated carbon. For example, You et al. synthesized activated carbon fibres from industrial polyacrylonitrile waste. The resulting material had a surface area of 2400 m^2/g and a porous volume of 1.15 cm^3/g, making it highly effective for adsorbing dyes from wastewater [14]. Such studies highlight the potential for using waste products to create new materials for water treatment, reducing the waste disposal burden at the same time. Other polymers, from natural or waste sources, have already been applied in water remediation procedures: Qu et al. developed a cotton-based material impregnated with chitosan for removing gold from water, demonstrating a strong interaction between the material and the metal [15,16]. Similarly, Rajakovic et al. created a sorbent from recycled wool for treating water contaminated by heavy oils, showing excellent adsorption properties comparable to commercial products [17].

Cigarette butts, which are one of the most widely produced and improperly discarded waste items, present a significant environmental challenge [18]. It is estimated that cigarette butts account for around 30 % of global waste, with roughly 6 billion cigarettes smoked worldwide every year [19]. Improper disposal of cigarette butts leads to the release of over 7000 harmful chemicals into the environment, including heavy metals like chromium, and lead as well as carcinogens such as polycyclic aromatic hydrocarbons [20]. Another issue stemming from improper cigarette butt disposal arises from the fact that cigarettes, in addition to being made of paper and tobacco, also contain polymeric/plastic materials, such as adhesive glues and the filter (primarily composed of cellulose acetate (CA)), which exhibit poor biodegradability in natural environments [21,22] with degradation times exceeding thirty years [20]. The problem of CA pollution has led to different recycling strategies to prepare sustainable materials of interest in several relevant sectors, such as construction (bricks, concrete, asphalt), acoustics (sound-absorbing materials), electronics (conductive materials, batteries), and chemistry (sorbent materials) [23].

Exploring recycling strategies in the literature, several studies describe procedures that transform cigarette butts into sorbent materials for water treatment [24]. Specifically, considering that the primary polymer, CA, has a high carbon atom content, cigarette butts are often used to synthesize carbon-based materials with strong sorbent capabilities, especially toward metal ions and inorganic pollutants [25,26]. However, the literature reveals that applications for removing water contaminants are limited to a narrow range of substances, such as heavy oils, metal ions, and dyes and not explored in depth [27–30]. Considering that water contamination also involves organic substances (emerging organic contaminants, EOCs), studies in this specific field are of pivotal importance to ensure high water protection [31].

In light of these considerations, this study proposes the synthesis of a new sustainable sorbent from CA recovered from cigarette butts and its application in water remediation application via flow through adsorption mode [32] toward common organic contaminants encountered in environmental water. The work is structured into three main phases: the recovery of the polymer, its transformation into a new composite sorbent material, and its application in water decontamination from EOCs [33]. The preparation process involves an accurate washing procedure of CA recovered from cigarette filters and the preparation of a composite sorbent material via an emulsion solidification technique, using activated carbon as a filler to improve the adsorption capability. The composite microbeads were characterized using scanning electron microscopy (SEM) and attenuated total reflectance Fourier-transform infrared spectroscopy (ATR-FTIR) to assess morphology and surface properties. The material applicability in removing a wide range of contaminants (pharmaceuticals, hormones, herbicides, pesticides, and fungicides) from natural waters was tested by designing an experimental setup (a glass cartridge packed with the sorbent microbeads and working in flow-through-mode) to simulate the water treatment operation. The adsorption dynamics of forty model compounds, characterized by different molecular weights, logP, and pKa, was evaluated using the model of the breakthrough curves, by fitting the experimental data with the Gompertz function [34,35]. A quantitative evaluation was also performed to estimate the overall retained quantity of each contaminant, having defined a saturation limit, a key parameter for defining the sorbent performance and benchmark for commercially available materials. We believe this study fills a large gap in the scientific literature and contribute to valorizing the harmful waste of cigarette butts in a valuable sorbent for water remediation. To our knowledge this is the first work of recovered CA-based sorbent material, produced from discarded cigarette butts, applied in flow-through adsorption mode for the removal of such a number of organic contaminants.

2. Materials and methods

2.1. Reagents and chemicals

Most of the standards for the target analytes (butoxycarboxim, methomyl, sulfaguanidine, sulfamerazine, pirimicarb, sulfamonomethoxine, sulfachloropyridazine, dimethoate, picloram, sulfathiazole, sulfamethoxazole, butocarboxim, prednisolone, thifensulfuron-methyl, propoxur, dexamethasone, cinosulfuron, metsulfuron-methyl, chlorsulfuron, carbaryl, atrazine, isoproturon, metobromuron, 2,4-dichlorophenol, 2,4-dichlorophenoxyacetic acid, naproxen, testosterone, flamprop, me-testosterone, linuron, desmedipham, phenmedipham, nimesulide, ibuprofen, procymidone, phenylbutazone, progesterone and iprodion) were purchased from Merck Life Science S.r.l. (Milan, Italy). Malathion and acephate were obtained from Dr. Ehrenstorfer GmbH (Wesel, Germany). **Table S1** of the **Supplementary material** presents the main chemical characteristics and structures of the forty target analytes.

Methanol (MeOH, purity > 99 %) and absolute ethanol (EtOH, purity > 99 %) were obtained from VWR International (Radnor, PA, USA); tetrahydrofuran (THF) and acetonitrile (RS-PLUS grade, purity 99.95 %) were purchased from Merck Life Science S.r.l. (Milan, Italy); water was generated by the MilliQ "Direct-Q® 3 UV system" manufactured by Merck KGaA (Darmstadt, Germany); formic acid (HCOOH, purity > 98 %) was acquired from Acros Organics B.V.B.A. (Waltham, MA, USA). Activated carbon was purchased from Special Ingredient Europe (Utrecht, Netherlands); sodium chloride (≥ 99 %) and n-dodecylamine (≥ 99 %) were acquired from Merck KGaA (Darmstadt, Germany).

2.2. Preparation of the working solutions

The standard solutions of the target analytes were prepared from individual commercial standards, with a purity grade greater than 99 %. The powders were weighed using a precision analytical balance (Ohaus DV215CD Discovery semi-micro and analytical balance, capacity 81/210 g, resolution 0.01/0.1 mg), transferred into volumetric flasks, and individually solubilized in MeOH. This process yielded stock solutions at 1 mg mL^{-1}, which were placed in amber vials and stored in a freezer at −18 °C. The working standard solution for testing water remediation performance was prepared by diluting the stock solutions in MilliQ water to a concentration of 0.5 mg l^{-1}.

2.3. Regeneration and characterization of cellulose acetate from cigarette stubs

Cigarette butts were collected from designated receptacles located in common spaces of Sapienza University of Rome. Once taken in laboratory, CA filters were recovered after removing paper, tobacco, and ash residues. Afterwards, approximately 3 g of cigarette filters were

weighed, placed into a beaker, and submitted to a washing procedure to remove combustion by-products. Under magnetic stirring, two washing steps were performed first with 10 mL of hot MilliQ water (90–100 °C) and then with 10 mL of EtOH. Finally, the clean filters were dried at 48 °C for approximately 40 min. For comparative analysis, cellulose acetate (CA) solutions (0.5 % w/v in acetone) were prepared from pristine, clean, and unwashed cigarette filters and characterized using UV–VIS spectrophotometry, ATR-FTIR and thermogravimetric analysis. For instrumental conditions, refer to Section 2.5 and **Section S1**. The results, presented in **Fig. S1, S2** and **S3**, demonstrate that the washing procedure effectively preserves the polymeric matrix, with the recovered material exhibiting fully comparable physicochemical and thermal properties to the pristine CA [24].

2.4. Preparation of cellulose acetate microbeads

The synthesis of the recycled sorbent material was conducted via microemulsion solidification of an organic solution of the polymer with a saturated aqueous solution of NaCl and dodecyl amine. The organic solution (dispersed phase) was prepared by dissolving 560 mg of washed filters in 10 mL of THF (5.6 % w/v) under gentle stirring for 2 min. Separately, a saturated solution of NaCl in MilliQ water and a 2 % n-dodecylamine solution were prepared and mixed in a 1:1 (v/v) volumetric ratio to create the dispersing solution. Then, 10 mL of this dispersing solution was added, under magnetic stirring (200 rpm), to 10 mL of the polymer organic solution to induce salting-out and form an emulsion. To break the microemulsion and promote the solidification of CA as microspheres, 11 mL of MilliQ water was added dropwise. At the end of the process, the system and the precipitation were stabilized by the addition of 10 mL of EtOH. The precipitate was then filtered using a vacuum pump, washed three times with 5 mL of MilliQ water and once with EtOH (5 mL per washing step) to remove unreacted materials and residual organic solvent. The synthetic procedure is displayed in Fig. 1.

A similar procedure was followed for synthesizing composite materials, in which a known quantity of activated carbons was dispersed in the organic phase after dissolving the polymer. As regards the final optimized material, 112.20 mg of activated carbon were added to produce a 20 % w/w composite (CA@AC-20 %). Other composites were synthesized by varying the percentage of activated carbon to study the performance trends: 5 % (CA@AC-5 %) and 10 % (CA@AC-10 %).

2.5. Characterization of the composite microbeads

The composite microbeads were characterized in terms of dimensional and morphological properties using SEM (model AURIGA; Carl Zeiss, Oberkochen, Germany). Prior to imaging, all samples were dried and coated with chromium to make their surfaces conductive. Micrographs were collected at various magnifications (100–1000 X), using a

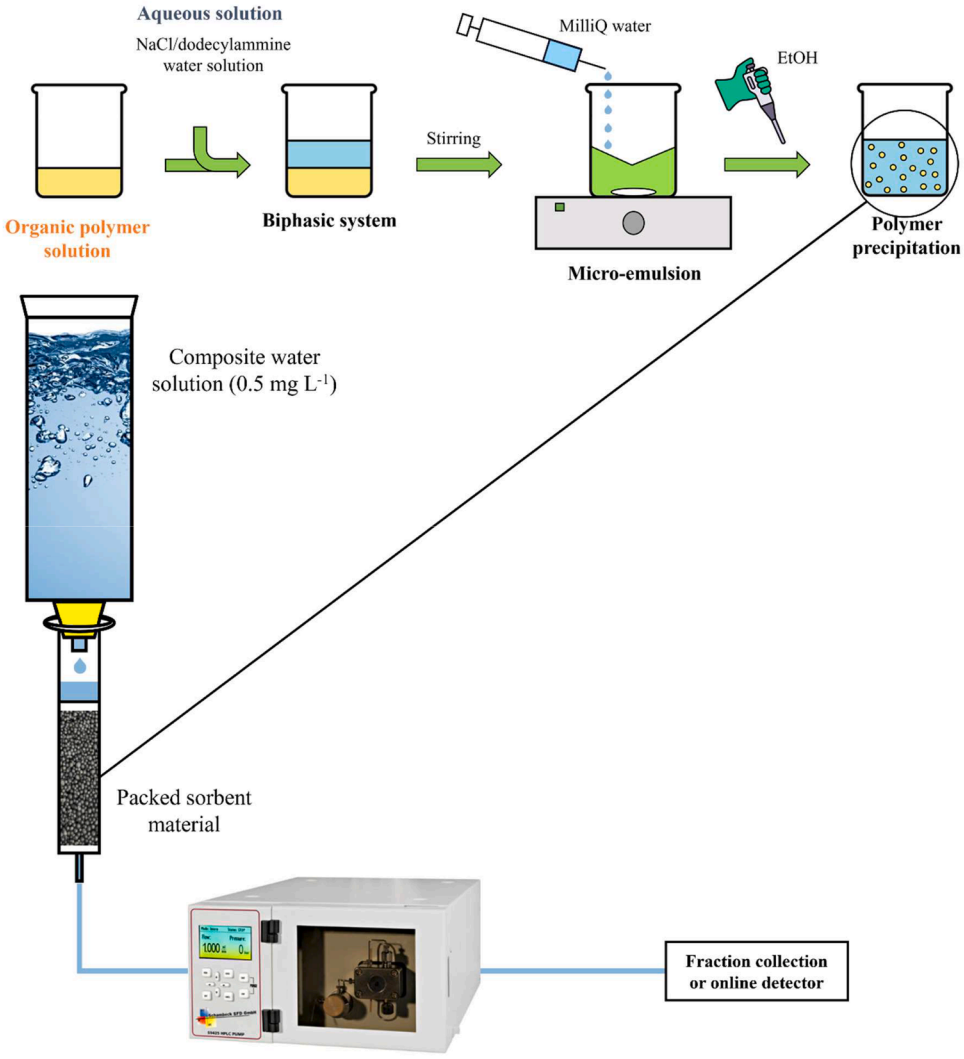

Fig. 1. Synthetic strategy of the new sorbent material and instrumental setup: a chromatographic pump sustains a dynamic flow of a water solution, spiked with all the 40 contaminants at 0.5 mg l^{-1}, inside the cartridge packed with the microbeads.

working distance of 14 mm, an electron accelerating voltage of 15 kV, and DISS for digital image acquisition.

A characterization study via ATR-FTIR was carried out using a Nicolet 6700 instrument (Thermo Fisher Scientific, Waltham, PA, USA), equipped with a Golden Gate single-reflection diamond accessory, with a resolution of 2 cm^{-1} over a spectral range of 400–4000 cm^{-1}, and co-addition of 200 scans.

2.6. Instrumental setup and optimization of the process conditions

To test the adsorption capability of the synthesized material, an instrumental setup was assembled to purify environmental water on a laboratory scale. A total of 40 common environmental contaminants were used as model compounds and their multi-standard solution (see Section 2.2) was used to spike 500-mL of MilliQ water at 0.5 mg l^{-1}. The aqueous sample was flowed through a glass cartridge filled with a known amount of synthesized composite microspheres (CA@AC-20 %), packed between two polypropylene frits. Specific constant flow rates were controlled by an HPLC pump (1260 Infinity II, Agilent Technologies, Inc., Milano, Italy). The instrumental setup is represented in Fig. 1.

To define optimal process parameters (flow rate, amount of sorbent, percentage of the activated carbon in the composite material), an experimental design was conducted by processing data with Statgraphics Centurion XV software (StatPoint, Inc., Warrenton, VA, USA). Through a relatively limited number of experiments designed to represent the process parameter variability (9 different experiments, each one made in triplicate for a total of 27 trials), response surfaces could be generated to model the performance of the contaminant removal process as a function of the considered variables. After selecting the process variables crucial in affecting the process performance, other preliminary steps in constructing the experimental design were: *i*) determination of reasonable experimental ranges for the identified variables, and *ii*) definition of desirability parameters to quantitatively define the process efficiency.

As above-mentioned, the process variables selected were: flow rate (X1), amount of sorbent material (X2), and the percentage of activated carbon within the composite (X3). The chosen experimental ranges for these variables were 0.25 – 1 mL min^{-1} for X1, 100–500 mg for X2, and 5–20 % for X3. As indicators of the purification level, spectrophotometric responses were recorded for two 500 μL aliquots of the cartridge eluting solution, collected after 10 min (Y1) and 60 min of processing (Y2). These aliquots were directly injected (100 μL) into an HPLC-UV (1260 Infinity II, Agilent Technologies, Inc., Milano, Italia), working in flow injection analysis under isocratic mode (100 % MilliQ water) at a flow rate of 1 mL min^{-1}; the signal was recorded at a wavelength of 230 nm (a good compromise for all the analytes). The analytical output was the area of the chromatographic peak of all analytes (an integrated signal), coeluting after some seconds from the injection due to the absence of a chromatographic column. This signal facilitates the monitoring of the overall removal process, offering comprehensive insights into the ongoing adsorption dynamics.

Among the various experimental designs reported in the literature, a face-centred experimental design was adopted. This involved eight independent experiments, conducted by setting the process variables to the extremes of the chosen experimental ranges, and one experiment with the process variables set at the central value within the range. By representing each variable as a Cartesian axis, the experiments conducted appear as points in space, distributed at the vertices and centre of a cube that circumscribes the space of possible variable combinations.

The results obtained in terms of recorded observables were used to establish the optimal functional relationship between the process variables and the observables themselves, fitting the data with the following equation:

$$y = b_0 + b_1X_1 + b_2X_2 + b_3X_3 + b_{12}X_1X_2 + b_{13}X_1X_3 + b_{23}X_2X_3 + b_{11}X_1^2 + b_{22}X_2^2 + b_{33}X_3^2$$

Upon defining the process variables, their ranges, and the observables, the experimental matrix was generated using the aforementioned software. All experiments were performed in triplicate to develop a robust and reliable model, resulting in a total of 27 experiments. Final conditions for the considered parameters were established as follows: $X1 = 0.25$ mL min^{-1}, $X2 = 500$ mg, $X3 = 20$ %.

2.7. Breakthrough curves

After optimizing the process parameters for the definition of the best operative conditions, the above-described instrumental setup was directly coupled with an online UV detection system ($\lambda = 230$ nm) to monitor in real-time the concentration changes in the solution eluting from the cartridge as a function of flushing time. Signal acquisition occurred from $t_0 = 0$ min, corresponding to the initial contact of the sorbent material in the cartridge with the contaminant solution, up to $t_{fin} = 30$ min. The trend of the spectroscopic signal (proportional to the overall concentration of contaminants in the solution), as a function of time, is referred to as the breakthrough curve. Specifically, this function reflects the integrated retention behaviour of all analytes in the cartridge.

To extract information on the individual analytes, breakthrough curves were obtained under the same treatment conditions by coupling the packed cartridge with a selective detection system, such as a mass spectrometer. To monitor the concentration trend of a specific analyte over time, the cartridge effluent was analysed using UPLC-MS/MS instrumentation (ACQUITY UPLC H—Class PLUS system, Waters Corporation, Milford, MA, USA), targeting specific ion transitions. The resulting breakthrough sigmoid reveals the retention behaviour of each analyte with the sorbent.

In this case, it was not feasible to directly couple the packed cartridge with the UPLC-MS/MS detection system online. Therefore, effluent fractions were collected at two-minute intervals, transferred into vials, and analysed via UPLC-MS/MS over a total analysis time of 30 min. The tracked signal was the chromatographic peak area associated with the ion transition of each analyte. Instrumental responses were plotted against flushing time, and the data points in the chromatographic area/time space were fitted to the Gompertz sigmoid function, defined as:

$$f(x) = d + (a - d)\cdot e^{-e^{-b\ \cdot\ (x-c)}}$$

From the Gompertz function providing the best fit for the experimental data, it was possible to extrapolate relevant information on the adsorption dynamics for each analyte. In fact, the Gompertz function, used to model the variation in recorded signals as a function of process time, is parameterized by four coefficients, each with a specific mathematical significance. The factors **d** and **a** represent the ordinate values to which the function asymptotically converges at 0 and $+\infty$, respectively. The constant ***c*** corresponds to the abscissa of the inflection point, while the coefficient **b** indicates the slope of the curve in the region of rapid growth. Each of these parameters takes on different values for each analyte, defining distinct adsorption dynamics in terms of saturation time, magnitude, and speed at which the asymptotic value is reached. This variability can be attributed to differential retention behaviour on the material due to the different the analyte properties.

To provide a physicochemical interpretation of the results, logP, molecular weight, and pKa were plotted against Gompertz's coefficients and saturation times at 10 % and 90 % of the active sites (see Section 3.2).

2.8. Ultra-Performance liquid chromatography coupled with tandem mass spectrometry (UPLC-MS/MS)

To analyse the collected fractions using UPLC-MS/MS instrumentation, it was essential to optimize a separation procedure ensuring the simultaneous quantification of all the analytes. Chromatographic separation was performed using an ACQUITY UPLC H—Class PLUS® system (Waters Corporation, Milan, Italy). Analyte separation was conducted in reverse-phase mode on an XTerra C18 column (2.1 × 150 mm, 3.5 μm) at a flow rate of 0.2 mL/min. Elution was carried out in a gradient mode with Milli-Q water containing 5 mM HCOOH (phase A) and acetonitrile containing 5 mM HCOOH (phase B) as the mobile phases. At t_0 phase B was 20 % and it was increased to 80 % in 20 min; this percentage was kept for 10 min, for a total run time of 30 min.

The detection was carried out by an API 4000 tandem mass spectrometer (AB Sciex, Foster City, CA, USA), equipped with a Turbo V source featuring an electrospray ionization (ESI) probe; detection was performed in dual polarity mode. The tandem mass spectrometry (MS/MS) settings were: capillary voltage of +5000 V for positive polarity, and −4500 V for negative polarity, air nebulizer gas at 2 L/min, drying gas (air) at 450 °C and 20 L/min, nitrogen curtain gas at 5 L/min, and nitrogen collision gas at 4 mTorr. The full width at half maximum (FWHM) was set at 0.7 ± 0.1 *m/z* in each mass-resolving quadrupole to maintain unit resolution. Analyst® Software version 1.5 was used for data acquisition and processing. For each analyte, **Table S2** shows the mass spectrometric and chromatographic parameters: precursor ion (Q1), product ions (Q3), declustering potential (DP), entrance potential (EP), collision energy (CE), collision cell exit potential (CXP) and retention time.

3. Results and discussion

3.1. Characterisation of regenerated material

The washing procedure, described in Section 2.3, allowed one to clean cigarette filters and to restore a material similar to the pristine CA. The effectiveness of the washing protocol and the final characteristics of the clean material were verified by the characterization carried out by UV–Vis spectroscopy, ATR-FTIR, and thermogravimetric analysis (TGA). A detailed discussion on the results, displayed in **Fig. S1**-**S3**, is reported in **Section S1** of the Supplementary Material.

3.2. Optimization of the synthetic strategy

Once the efficiency of the washing procedure was confirmed, a synthetic strategy was developed to produce a new sorbent material. The process variables chosen to optimize the synthetic procedure were: amount of polymer in solution, percentage of activated carbon in the final material, magnetic stirring speed, volume of Milli-Q water added during microemulsion breakage. The factors taken into account to evaluate the suitability of the final product included the distribution of microbead size, stability, and yield. Dimensionality and shape uniformity are among the most critical parameters for water remediation applications in flow-through mode, as they directly influence packing quality and, consequently, the efficiency of the purification process itself. Non-uniform material or particles that are excessively large or small can result in undesirable outcomes, such as: *i*) formation of multiple or preferential flow paths, leading to poor interaction between analytes and the material, and therefore, suboptimal water purification; *ii*) excessive back pressure, making the process energetically costly to facilitate water flow through the device.

To optimize the synthetic procedure, process variables were selected within a reasonable range. Three distinct levels were chosen for each parameter, resulting in an experimental matrix of 81 trials. Each synthetic trial was given a score to determine the best operating conditions and finalize the synthetic workflow. The values selected for each parameter are displayed in **Table S3**. The final optimized conditions are those detailed in the synthetic procedure described in Section 2.4.

3.3. Characterization of microbeads

3.3.1. SEM micrographs

SEM analyses were performed to investigate the morphology and size of the materials synthesized in form of microbeads (CA, CA@−20 %). The two panels **a** and **b** in Fig. 2 respectively show polymeric microspheres with a homogeneous composition of pure CA and its composite with activated carbons, which enhance adsorption yields. The images were captured at magnifications of 100X and 189X, respectively. In both cases, the CA-based microbeads appear to be reasonably monodispersed, with average diameters of approximately 200 μm.

3.3.2. ATR-FTIR spectra collection

ATR-FTIR analyses revealed that the spectra of commercial and recovered CA are almost superimposable (Fig. S2). These results reveal the recovery procedure is not responsible for a relevant degradation of the polymeric material. On the other hand, the activated carbons do not cause significant changes in the FTIR transmittance spectrum of the synthesized material (CA@AC-20 %) compared to pristine CA (Fig. 2), demonstrating the capability of the synthetic strategy to deeply incorporate the additive within the sorbent. For an accurate identification of IR bands refer to Section S1 of the Supplementary material.

3.4. Optimization of the instrumental workflow

Having confirmed that the material meets all the required criteria in terms of shape, size distribution, and stability, its applicability was evaluated. To assess the retention behaviour of the 40 selected contaminants under dynamic conditions, a glass cartridge was packed with a known quantity of the microbeads CA@AC-20 %. A composite solution at a known concentration (0.5 mg l^{-1} of each analyte) was used as the test solution to evaluate the material adsorption abilities, in competitive mode. To optimize the critical parameters of the planned instrumental setup, an experimental design approach was employed. Details on the model type and parameters selected are provided in Section 2.6. Table 1 reports the experimental matrix generated by the software. Each experiment, represented by a row in the table with its corresponding process conditions, was conducted in triplicate. For each experiment, mean values of the observables Y_1 and Y_2 were tabulated. From the mathematical fit of the experimental data, the response surface was obtained (Fig. 3).

It was observed that, fixing X_1 at 0.25 mL/min, desirability increased upon rising values of the process variables X_2 and X_3. Optimal water treatment conditions were achieved at 0.25 mL/min using 500 mg of sorbent material doped with 20 % activated carbon, resulting in a maximum desirability value of 0.707. Higher flow rates led to a faster leakage of the analytes, which can be explained by insufficient interaction time with the active sites of the sorbent.

3.5. Breakthrough curves

Once the optimal process conditions for the instrumental setup were established, the study of the sorbent retention capabilities was conducted. To this end, breakthrough curves related to the adsorption process of analytes were built. Depending on the experimental requirements, the integrated content of both all the analytes and the individual species at the cartridge outlet was monitored.

Following the overall concentration of the contaminants in the effluent solution, the breakthrough curve presented in Fig. 4 was built. The sigmoid trend is typical of breakthrough curves for homogeneous solid sorbent materials. From the experimental trend, it was possible to drawn time values for the saturation of 10 and 90 % of the total available adsorption sites of the packed material. As an average on five replicates,

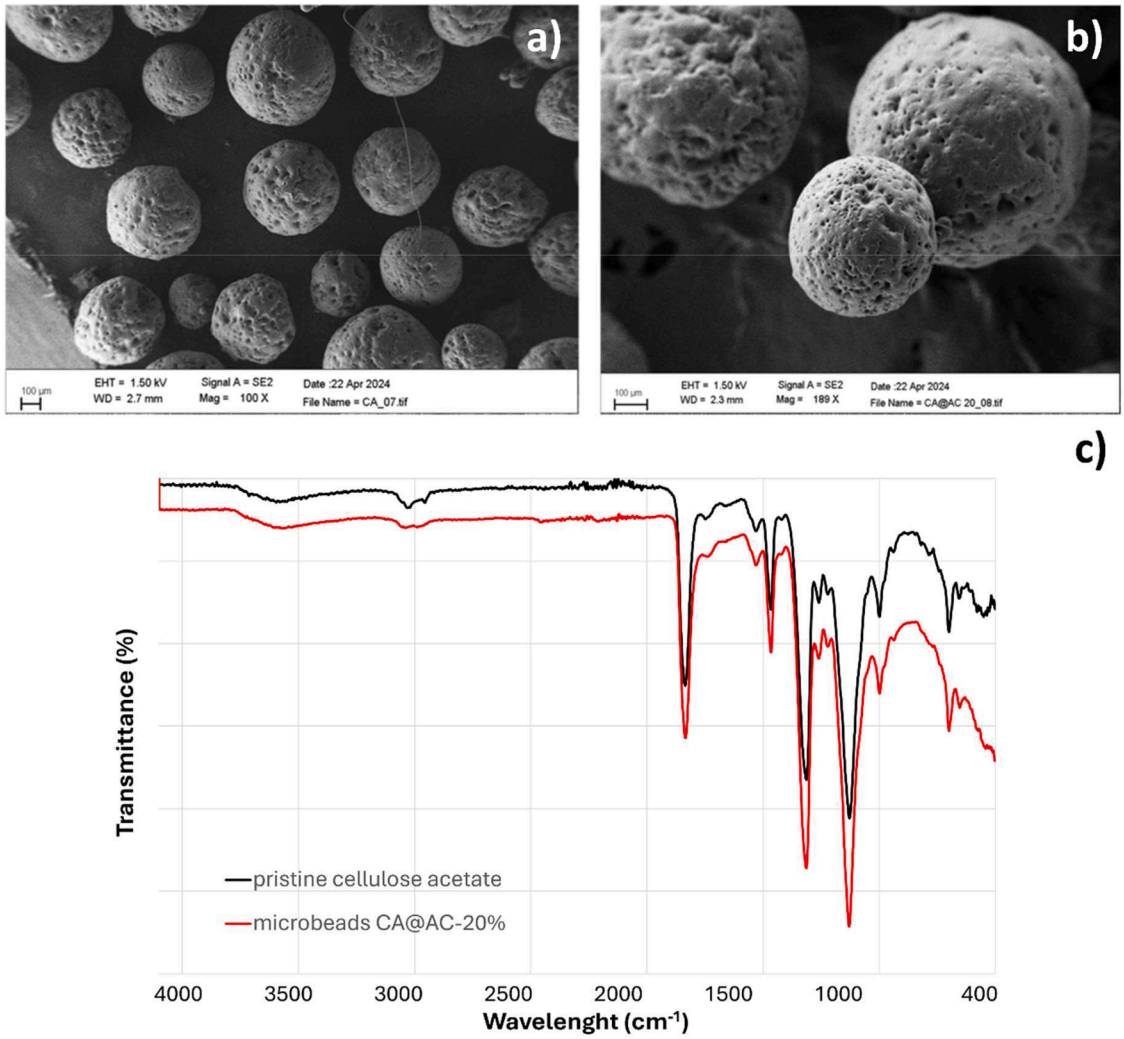

Fig. 2. SEM images and FTIR spectra (shifted) of both microspheres composed solely of cellulose acetate (CA) (panel **a** and black spectrum) and composite microspheres (CA@−20 %) (panel **b** and red spectrum).

Table 1
Experimental matrix for the optimization of setup parameters (X1 = flow rate, X2 = active carbons amount, X3 = microspheres amount).

X1 (mL min^{-1})	X2 (mg)	X3 (% w/w)
0.625	300	12.5
0.25	500	5
1	100	20
0.25	500	20
1	500	5
1	100	5
0.25	100	20
0.25	100	5
1	500	20

the saturation times for the 10 and 90 % of saturation are 9.12 ± 0.03 min and 30.96 ± 0.08 min, respectively.

As described in Section 2.7, breakthrough curves for each analyte were recorded under the same process conditions using an offline connection between the cartridge and the mass spectrometer detector. Based on the developed method, the limits of detection (LODs) for the analytes were calculated. These LODs serve as threshold values, meaning the material's removal effectiveness could only be assessed for concentrations at or above these limits. The LODs range from 0.2 to 14.2 μg/L, enabling the detection of analytes at environmentally relevant concentrations and allowing for the assessment of their removal even at low contamination levels. Instrumental features and performances of the detection method for each analyte are reported in **Table S4** of the Supplementary material. Gompertz function was used to fit the experimental data for single analyte, returning a sigmoid trend parameterized by the coefficients defined in Section 2.7. Fig. 5 presents the breakthrough curves for the adsorption process on the composite microspheres, along with the 10 % and 90 % saturation times of active sites for three representative analytes from each of the five contaminant classes.

Saturation times are directly proportional to the availability of the sorbent active sites for each analyte. Lipophilic analytes tend to interact more effectively with the material compared to polar analytes, although the contribution of functional groups on a molecule and their spatial arrangement within the chemical structure must also be considered. Another key parameter defining the retention capabilities of the material with respect to the analytes is represented by the coefficients c and a of the Gompertz function, which provides the best fit to the experimental data. All the coefficients of the Gompertz functions that best fit the experimental breakthrough trends of the analytes are reported in Table 2, along with saturation times. As a measure of goodness of fit, the coefficient of determination (R^2) is reported for the trends provided for each of the analytes. To establish a correlation between these experimental parameters and the physicochemical properties of the analytes, they were plotted against logP, pKa and molecular weights of the

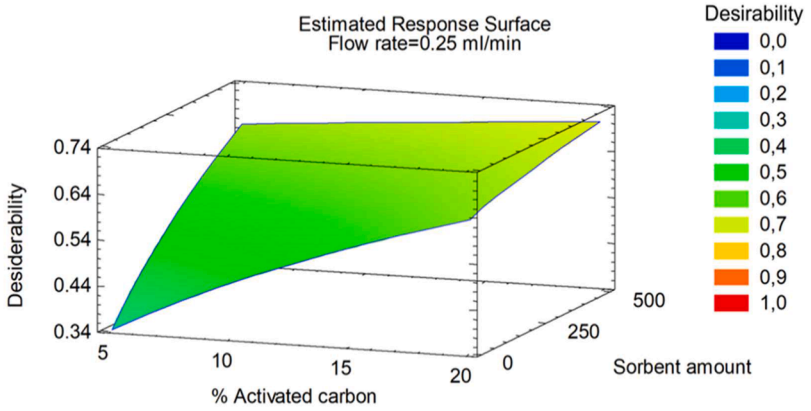

Fig. 3. Surface response of the experimental design obtained by fixing the experimental variable X1 (flow rate) to the fixed value of 0.25 mL min^{-1}.

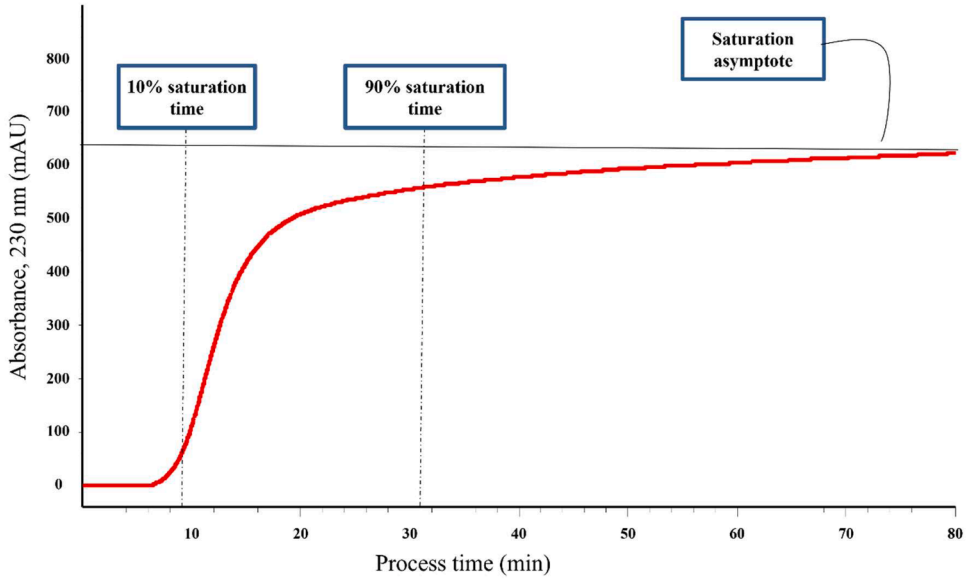

Fig. 4. The breakthrough curve integrated across all the analytes; times corresponding to 10 % and 90 % saturation of the active sites within the packed cartridge are highlighted.

analytes. The best correlation is provided by following the trend of the coefficient c of the Gompertz function against the logP value of the analytes (see Fig. 6). The coefficient c of the Gompertz function varies proportionally as the logP values increase, following an approximately exponential trend. A sudden rise in the inflection points of the breakthrough curve is observed for logP values greater than 3.

To provide quantitative data on the material retention capacity, the amount of each analyte retained by the sorbent under saturation conditions was estimated. This information was extrapolated from the breakthrough curves of the individual analytes through geometric considerations. The area under the breakthrough sigmoid represents the amount of analyte that was not retained by the cartridge but instead passed through the material and was detected by the spectrophotometer. A 30-min interval was chosen as a secure temporal threshold, within which the sorbent's active sites can be considered saturated for all analytes, with their respective breakthrough curves reaching a *plateau*. Integrating the sigmoid from 0 to 30 min, an estimate of the total amount of analyte not retained by the cartridge during this time is provided. By subtracting this area from the integral of the saturation asymptote over the same interval, the resulting area reflects the amount of analyte retained by the material under competitive saturation conditions. This area value can then be converted into the quantity of analyte, expressed in nanograms, using a multiplicative constant **k**. This constant represents the relationship between the area unit and the analyte quantity, and is calculated as the ratio of the area between the asymptotes over a time interval Δt to the amount of analyte passing through the cartridge in the same time interval. The multiplicative factor **k** transforms an area into an estimate of the amount of analyte retained in the cartridge. The analytes amounts retained by the cartridge under saturation conditions (30 min) are reported in Table 2. As a result of these quantitative considerations, the material is able to adsorb a total amount of contaminants on the order of 125 μg per gram, in competitive mode, by using a dynamic retention strategy.

3.6. *Stability and reuse of composite microbeads*

The shelf life of a product is crucial for its possible industrial uses. The possibility of using the material long after its preparation is a characteristic that increases its appeal in industrial processes and expands its potential applications. This study explores the stability of the material after some months from the synthetic process and the performance of it in the adsorption process. For this reason, breakthrough curves have been collected in the same conditions after 6 months from the preparation, by storing the material at room temperature, protecting it from thermal and physical stress. To give an idea of the stability and reproducibility of the result, the comparison of the integrated

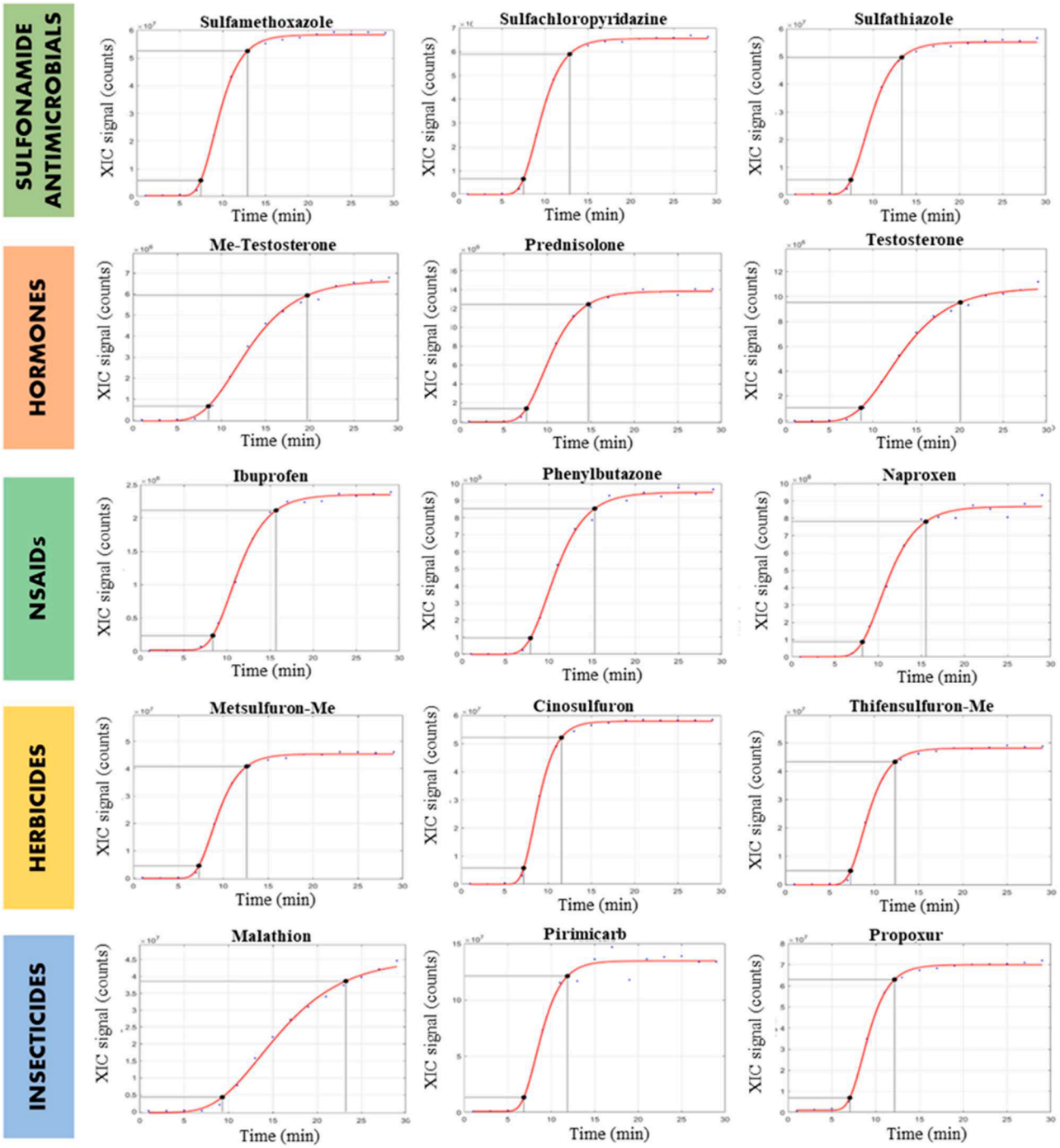

Fig. 5. Breakthrough curves of three representative analytes from each of the five classes of contaminants: sulfonamide antimicrobials, hormones, NSAIDs, herbicides and insecticides.

breakthrough collected after six months, with material from the same synthesis batch, is shown in **Fig. S4** of the Supplementary material. The deviation observed between the collected curves was less than 15 %, without showing a significant decrease in the material's performance.

Activated carbons are widely used as adsorption additives in techniques and materials for water remediation. One of the main challenges associated with their application is the possibility of reuse. Two primary regeneration strategies for activated carbons have been reported in the literature. By either desorbing or decomposing the adsorbed chemical species, the material can be recovered in its original form, with varying effectiveness depending on the specific technology used [36]. In general, desorption is the most widely adopted method, as it does not require hazardous reagents that could pose environmental concerns [37]. However, solvent desorption, to the best of our knowledge, presents several drawbacks, including the aggressiveness of the solvents used, the poor reversibility of the adsorption process on activated carbon, and the relatively low recovery yields, often below 70 %. For these reasons, thermal desorption is more commonly employed. While its efficiency depends on the specific type of activated carbon used, it generally provides higher desorption yields and reduces the need for additional chemical reagents. Thermal desorption is typically conducted at elevated temperatures ranging from 700 °C to 1000 °C, using either inert gases or controlled amounts of oxidizing gases, such as steam or flue gas. Treating cellulose acetate microspheres under these conditions results in

Table 2
Gompertz coefficients, saturation times, retained amount and determination coefficient related to the best model that fits the adsorption profile of each analytes.

	Analytes	Coefficient a of the Gompertz function	Coefficient b of the Gompertz function	Coefficient c of the Gompertz function	Coefficient d of the Gompertz function	10 % saturation time (min)	90 % saturation time (min)	Retained amount (μg)	R^2
1	Acephate	$2.71 \cdot 10^7$	0.6	8.6	$3.51 \cdot 10^5$	7.0	12.6	1.19	0.991
2	Butoxycarboxim	$1.01 \cdot 10^7$	0.6	8.8	$1.69 \cdot 10^5$	7.2	12.6	1.20	0.998
3	Methomyl	$7.66 \cdot 10^7$	0.4	9.2	$-2.11 \cdot 10^5$	7.1	14.7	1.32	0.998
4	Sulfaguanidine	$1.62 \cdot 10^7$	0.4	9.4	$2.24 \cdot 10^4$	7.5	14.4	1.33	0.995
5	Sulfamerazine	$3.05 \cdot 10^7$	0.4	8.5	$1.62 \cdot 10^5$	6.6	13.6	1.22	0.997
6	Pirimicarb	$1.44 \cdot 10^8$	0.6	8.7	$1.75 \cdot 10^6$	7.2	12.4	1.19	0.986
7	Sulfamonomethoxine	$9.95 \cdot 10^6$	0.3	10.0	$-3.79 \cdot 10^4$	7.5	16.9	1.47	0.997
8	Sulfachloropyridazine	$4.85 \cdot 10^7$	0.3	10.4	$-1.77 \cdot 10^5$	7.9	17.2	1.52	0.999
9	Dimethoate	$3.92 \cdot 10^6$	0.3	10.4	$-1.14 \cdot 10^4$	8.0	16.8	1.50	0.998
10	Picloram	$5.07 \cdot 10^6$	0.4	13.9	$-1.21 \cdot 10^3$	11.9	19.2	0.08	0.995
11	Sulfathiazole	$3.65 \cdot 10^7$	0.3	10.3	$-1.24 \cdot 10^5$	7.9	17.0	1.51	0.999
12	Sulfamethoxazole	$4.09 \cdot 10^7$	0.3	10.3	$-1.11 \cdot 10^5$	7.9	16.9	1.50	0.999
13	Butocarboxim	$2.16 \cdot 10^6$	0.5	9.4	$5.71 \cdot 10^3$	7.6	14.1	1.32	0.996
14	Prednisolone	$1.10 \cdot 10^7$	0.5	9.4	$7.32 \cdot 10^4$	7.7	13.6	1.30	0.999
15	Thifensulfuron-Me	$3.88 \cdot 10^7$	0.5	9.1	$2.65 \cdot 10^5$	7.5	13.4	1.90	0.998
16	Propoxur	$6.34 \cdot 10^7$	0.6	8.9	$5.82 \cdot 10^5$	7.5	12.6	1.48	0.999
17	Dexametasone	$5.59 \cdot 10^6$	0.3	10.0	$-5.81 \cdot 10^4$	7.6	16.9	1.24	0.992
18	Cinosulfuron	$5.26 \cdot 10^7$	0.6	8.6	$4.24 \cdot 10^5$	7.2	12.3	1.27	0.999
19	Metsulfuron-Me	$3.88 \cdot 10^7$	0.6	8.8	$2.93 \cdot 10^5$	7.3	12.9	1.23	0.999
20	Chlorsulfuron	$2.63 \cdot 10^5$	0.4	9.9	$2.15 \cdot 10^3$	7.8	15.5	1.19	0.952
21	Carbaryl	$1.18 \cdot 10^7$	0.2	14.8	$-1.02 \cdot 10^5$	9.6	24.6	1.65	0.995
22	Atrazine	$1.22 \cdot 10^5$	1.4	10.6	$3.63 \cdot 10^3$	10.0	12.2	1.41	0.991
23	Isoproturon	$1.67 \cdot 10^7$	0.3	11.3	$-9.09 \cdot 10^4$	8.3	19.4	1.23	0.995
24	Metobromuron	$2.44 \cdot 10^6$	0.2	14.5	$-2.07 \cdot 10^3$	10.1	23.8	1.89	0.992
25	2,4-Dichlorophenol	$9.75 \cdot 10^5$	0.2	12.5	$-9.49 \cdot 10^3$	8.7	21.8	1.80	0.998
26	2,4-Dichlorophenoxyacetic Acid	$2.27 \cdot 10^7$	0.2	12.1	$-1.86 \cdot 10^5$	8.7	20.9	1.58	0.999
27	Naproxen	$2.13 \cdot 10^6$	0.2	12.5	$-1.94 \cdot 10^4$	9.1	21.3	2.05	0.994
28	Testosterone	$8.20 \cdot 10^6$	0.2	12.4	$-5.44 \cdot 10^4$	9.0	21.0	1.35	0.997
29	Flamprop	$2.55 \cdot 10^7$	0.4	11.1	$-6.55 \cdot 10^4$	8.8	17.1	1.90	0.999
30	Me-Testosterone	$4.93 \cdot 10^6$	0.2	12.2	$-4.13 \cdot 10^4$	8.8	20.9	1.78	0.997
31	Linuron	$5.44 \cdot 10^5$	0.1	17.6	$-2.00 \cdot 10^3$	11.0	26.0	1.23	0.996
32	Desmedipham	$5.52 \cdot 10^5$	0.1	23.9	$3.77 \cdot 10^3$	13.6	27.4	1.76	0.956
33	Phenmedipham	$6.48 \cdot 10^5$	0.1	26.3	$2.47 \cdot 10^3$	13.8	27.6	1.94	0.968
34	Nimesulide	$3.44 \cdot 10^6$	0.1	18.2	$3.36 \cdot 10^3$	11.6	26.2	1.75	0.996
35	Ibuprofen	$9.01 \cdot 10^5$	0.2	14.3	$-4.34 \cdot 10^1$	10.2	23.4	1.79	0.999
36	Procimidone	$2.99 \cdot 10^5$	0.1	17.8	$-7.59 \cdot 10^2$	10.7	26.1	1.47	0.994
37	Malathion	$2.76 \cdot 10^7$	0.2	14.4	$-2.07 \cdot 10^5$	9.6	24.1	1.88	0.997
38	Phenylbutazone	$4.07 \cdot 10^5$	0.2	13.0	$-4.10 \cdot 10^3$	9.3	22.2	1.89	0.997
39	Progesterone	$2.33 \cdot 10^6$	0.2	18.0	$1.34 \cdot 10^4$	12.7	25.9	1.82	0.999
40	Iprodion	$3.48 \cdot 10^4$	0.2	16.2	$1.29 \cdot 10^2$	10.6	25.3	1.94	0.957

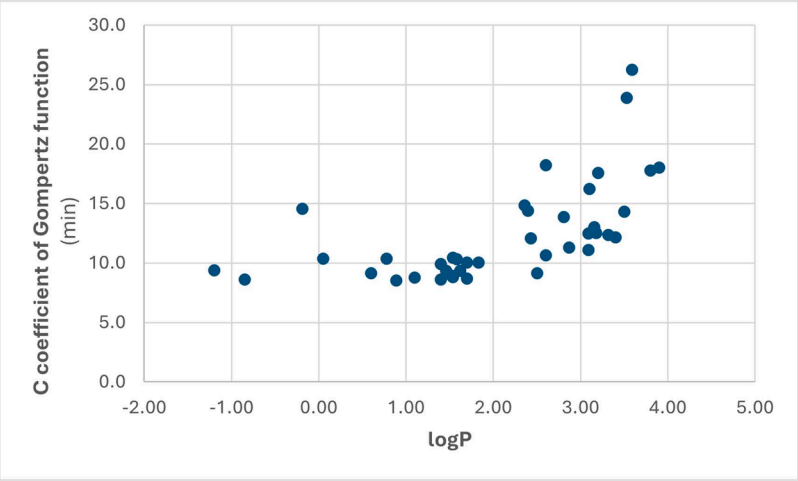

Fig. 6. Correlation of the c coefficient of the Gompertz function against the logP of the analytes.

the desorption of retained organic compounds and, simultaneously, the carbonization of the cellulose acetate support [38]. This process yields activated carbon through regeneration and recycling. The resulting material can be integrated into a new production process for composite microspheres, paving the way for a circular utilization approach with minimal waste generation.

4. Conclusions

Addressing water scarcity and pollution requires a multifaceted approach that includes better resource management, pollution prevention, and the development of new materials for water purification. The innovative use of natural and recycled materials in water remediation represents a crucial step toward a more sustainable future. In the current work new sorbent materials were synthesized from the bioplastic cellulose acetate, recovered from cigarette butts. The sorbents exhibited excellent qualities in terms of both performance and applicability, as well as environmental sustainability. They were found to be non-toxic, eco-friendly, and low-cost materials. Stability of the produced microbeads was tested, showing reproducible performances after six months from the preparation. A reusability workflow was displayed based on the already reported conditions of contaminants desorption and cellulose acetate carbonization, projecting the material into a virtuous economic cycle. Based on the obtained results, it was confirmed that these materials have good retention capacity for a wide range of contaminants, positioning them as a potential alternative to traditional and common sorbents used in water remediation applications. Based on these considerations, the prospects for the use and applicability of the newly synthesized sorbent materials appear particularly promising. Future objectives include exploitation of the reusability of the sorbent as described in Section 3.3 and the application of this approach to other polymers, the implementation of such materials to sample preparation methodologies and the possibility of a scale up of the process at an industrial level.

Funding

This work was supported by Sapienza University of Rome, Progetto di Avvio alla Ricerca 2024 (2024 Start-up research project), protocol number B83C24004910001, and Progetto di Avvio alla Ricerca 2022 (2022 Start-up research project), protocol number AR1221816C7498C6.

CRediT authorship contribution statement

Lorenzo Antonelli: Writing – original draft, Methodology, Conceptualization. **Susanna Grasso:** Writing – original draft, Investigation, Formal analysis. **Massimo Giuseppe De Cesaris:** Software, Funding acquisition, Data curation. **Nina Felli:** Visualization, Validation, Resources. **Chiara Dal Bosco:** Visualization, Supervision. **Stefano Cinti:** Supervision, Data curation. **Alessandra Gentili:** Writing – review & editing, Project administration.

Declaration of competing interest

The authors declare that they have no known competing financial interests or personal relationships that could have appeared to influence the work reported in this paper.

Supplementary materials

Supplementary material associated with this article can be found, in the online version, at doi:10.1016/j.greeac.2025.100283.

Data availability

Data will be made available on request.

References

[1] R.K. Mishra, Fresh water availability and its global challenge, Br. J. multidiscip. Adv. Stud. 4 (3) (2023) 1–78, https://doi.org/10.37745/bjmas.2022.0208.
[2] N.B. Singh, G. Nagpal, S. Agrawal, Water purification by using sorbents: a review, Environ. Technol. Innov. 11 (2018) 187–240, https://doi.org/10.1016/j.eti.2018.05.006.
[3] N. Akhtar, M.I. Syakir Ishak, S.A. Bhawani, K. Umar, Various natural and anthropogenic factors responsible for water quality degradation: a review, Water 13 (19) (2021) 2660, https://doi.org/10.3390/w13192660.
[4] S. Somma, E. Reverchon, L. Baldino, Water purification of classical and emerging organic pollutants: an extensive review, ChemEngineering 5 (3) (2021) 47, https://doi.org/10.3390/chemengineering5030047.
[5] H.H. Ngo, W. Guo, J. Zhang, S. Liang, C. Ton-That, X. Zhang, Typical low cost biosorbents for adsorptive removal of specific organic pollutants from water, Bioresour. Technol. 182 (2015) 353–363, https://doi.org/10.1016/j.biortech.2015.02.003.
[6] Á.I. López-Lorente, F. Pena-Pereira, S. Pedersen-Bjergaard, V.G. Zuin, S.A. Ozkan, E. Psillakis, The ten principles of green sample preparation, TrAC, Trends Anal. Chem. 148 (2022) 116530, https://doi.org/10.1016/j.trac.2022.116530.
[7] S. Armenta, S. Garrigues, M. de la Guardia, Green analytical chemistry, TrAC, Trends Anal. Chem. 27 (6) (2008) 497–511, https://doi.org/10.1016/j.trac.2008.05.003.
[8] I. Ali, New generation sorbents for water treatment, Chem. Rev. 112 (10) (2012) 5073–5091, https://doi.org/10.1021/cr300133d.
[9] J. Li, X. Dong, X. Liu, X. Xu, W. Duan, J. Park, L. Gao, Y. Lu, Comparative study on the adsorption characteristics of heavy metal ions by activated carbon and selected natural adsorbents, Sustainability, (2022) 14(23), 15579. doi:10.3390/su142315579.
[10] M.M. Sabzehmeidani, S. Mahnaee, M. Ghaedi, H. Heidari, V.A. Roy, Carbon based materials: a review of sorbents for inorganic and organic compounds, Mater. Adv. 2 (2) (2021) 598–627, https://doi.org/10.1039/D0MA00087F.
[11] M.S. Soffian, F.Z. Halim, F. Aziz, M.A. Rahman, M.A. Amin, D.N. Chee, Carbon-based material derived from biomass waste for wastewater treatment, Environ. Adv. 9 (2022) 100259, https://doi.org/10.1016/j.envadv.2022.100259.
[12] J.M. Dias, M.C. Alvim-Ferraz, M.F. Almeida, J. Rivera-Utrilla, M. Sánchez-Polo, Waste materials for activated carbon preparation and its use in aqueous-phase treatment: a review, J. Environ. Manag. 85 (4) (2007) 833–846, https://doi.org/10.1016/j.jenvman.2007.07.031.
[13] R.R. Bansode, J.N. Losso, W.E. Marshall, R.M. Rao, R.J. Portier, Adsorption of volatile organic compounds by pecan shell-and almond shell-based granular activated carbons, Bioresour. Technol. 90 (2) (2003) 175–184, https://doi.org/10.1016/S0960-8524(03)00117-2.
[14] S.Y. You, Y.H. Park, C.R. Park, Preparation and properties of activated carbon fabric from acrylic fabric waste, Carbon 38 (10) (2000) 1453–1460, https://doi.org/10.1016/S0008-6223(99)00278-X.
[15] D. Gomez-Maldonado, I.B. Vega Erramuspe, M.S. Peresin, Natural polymers as alternative sorbents and treatment agents for water remediation, Bioresour 14 (4) (2019), https://doi.org/10.15376/biores.14.4.gomez-maldonado.
[16] R. Qu, C. Sun, M. Wang, C. Ji, Q. Xu, Y. Zhang, C. Wang, H. Chen, P. Yin, Adsorption of Au (III) from aqueous solution using cotton fiber/chitosan composite sorbents, Hydrometallurgy 100 (1–2) (2009) 65–71, https://doi.org/10.1016/j.hydromet.2009.10.008.
[17] V. Rajakovic, G. Aleksic, M. Radetic, L. Rajakovic, Efficiency of oil removal from real wastewater with different sorbent materials, J. Hazard. Mater. 143 (1–2) (2007) 494–499, https://doi.org/10.1016/j.jhazmat.2006.09.060.
[18] P. Stigler Granados, L. Fulton, E. Nunez Patlan, M. Terzyk, T.E. Novotny, Global health perspectives on cigarette butts and the environment, Int. J. Environ. Res. Public Health 16 (10) (2019) 1858, https://doi.org/10.3390/ijerph16101858.
[19] T.E. Novotny, K. Lum, E. Smith, V. Wang, R. Barnes, Cigarettes butts and the case for an environmental policy on hazardous cigarette waste, Int. J. Environ. Res. Public Health 6 (5) (2009) 1691–1705, https://doi.org/10.3390/ijerph6051691.
[20] E. Slaughter, R.M. Gersberg, K. Watanabe, J. Rudolph, C. Stransky, T.E. Novotny, Toxicity of cigarette butts, and their chemical components, to marine and freshwater fish, Tob. Control 20 (Suppl 1) (2011) i25–i29, https://doi.org/10.1136/tc.2010.040170.
[21] J. Torkashvand, M. Farzadkia, H.R. Sobhi, A. Esrafili, Littered cigarette butt as a well-known hazardous waste: a comprehensive systematic review, J. Hazard. Mater. 383 (2020) 121242, https://doi.org/10.1016/j.jhazmat.2019.121242.
[22] T.E. Novotny, S.N. Hardin, L.R. Hovda, D.J. Novotny, M.K. McLean, S. Khan, Tobacco and cigarette butt consumption in humans and animals, Tob. Control 20 (Suppl 1) (2011) i17–i20, https://doi.org/10.1136/tc.2011.043489.
[23] H. Kurmus, A. Mohajerani, The toxicity and valorization options of cigarette butts, J. Waste Manag. 104 (2020) 104–118, https://doi.org/10.1016/j.wasman.2020.01.011.
[24] M.G. De Cesaris, N. Felli, L. Antonelli, I. Francolini, G. D'Orazio, C. Dal Bosco, A. Gentili, Recovery of cellulose acetate bioplastic from cigarette butts: realization of a sustainable sorbent for water remediation, Sci. Total Environ. 929 (2024) 172677, https://doi.org/10.1016/j.scitotenv.2024.172677.
[25] J. Ganster, H.P. Fink, Cellulose and cellulose acetate. Bio-Based Plastics: Materials and Applications, Wiley, 2013, pp. 35–62, https://doi.org/10.1002/9781118676646.ch3.
[26] M. Oprea, S.I. Voicu, Cellulose acetate-based materials for water treatment in the context of circular economy, Water 15 (10) (2023) 1860, https://doi.org/10.3390/w15101860.
[27] X. Zhang, M. Yu, Y. Li, F. Cheng, Y. Liu, M. Gao, G. Liu, L. Hu, Y. Liang, Effectiveness of discarded cigarette butts derived carbonaceous sorbent for heavy metals removal from water, Microchem. J. 168 (2021) 106474, https://doi.org/10.1016/j.microc.2021.106474.

[28] M. Oprea, S.I. Voicu, Cellulose acetate-based membranes for the removal of heavy metals from water in the context of circular economy, Ind. Crop. Prod. 206 (2023) 117716, https://doi.org/10.1016/j.indcrop.2023.117716.
[29] J. Uebe, T. Paulauskiene, K. Boikovych, Cost-effective and recyclable aerogels from cellulose acetate for oil spills clean-up, ESPR 28 (2021) 36551–36558, https://doi.org/10.1007/s11356-021-13369-9.
[30] P. Ananthi, K. Hemkumar, S. Manikandan, Cellulose acetate based-membrane supported by metal-organic frameworks for the removal of diclofenac and ciprofloxacin from polluted water, Groundw. Sustain. Dev. 26 (2024) 101308, https://doi.org/10.1016/j.gsd.2024.101308.
[31] W.M. Shackelford, D.M. Cline, Organic compounds in water, Environ. Sci. Technol. 20 (7) (1986) 652–657. https://pubs.acs.org/doi/pdf/10.1021/es00149a002.
[32] H. Patel, Fixed-bed column adsorption study: a comprehensive review, Appl. Water Sci. 9 (3) (2019) 45, https://doi.org/10.1007/s13201-019-0927-7.
[33] L. Antonelli, M.C. Frondaroli, M.G. De Cesaris, N. Felli, C. Dal Bosco, E. Lucci, A. Gentili, Nanocomposite microbeads made of recycled polylactic acid for the magnetic solid phase extraction of xenobiotics from human urine, Microchim. Acta 191 (5) (2024) 1–14, https://doi.org/10.1007/s00604-024-06335-y.
[34] M.A.E. de Franco, C.B. de Carvalho, M.M. Bonetto, R. de Pelegrini Soares, L. A. Féris, Removal of amoxicillin from water by adsorption onto activated carbon in batch process and fixed bed column: kinetics, isotherms, experimental design and breakthrough curves modelling, J. Clean. Prod. 161 (2017) 947–956.
[35] K.H. Chu, Fitting the Gompertz equation to asymmetric breakthrough curves, J. Environ. Chem. Eng. 8 (2020) 103713, https://doi.org/10.1016/j.jclepro.2017.05.197.
[36] O. Zanella, I.C. Tessaro, L.A. Féris, Desorption-and decomposition-based techniques for the regeneration of activated carbon, Chem. Eng. Technol. 37 (9) (2014) 1447–1459, https://doi.org/10.1002/ceat.201300808.
[37] F. Huang, W. Liu, S. Chen, Z. Tian, J. Wei, Thermal desorption characteristics of the adsorbate in activated carbon based on a two-dimensional heat and mass transfer model, Appl. Therm. Eng. 214 (2022) 118775, https://doi.org/10.1016/j.applthermaleng.2022.118775.
[38] J. Fischer, K. Thummler, S. Fischer, I.G. Gonzalez Martinez, S. Oswald, D. Mikhailova, Activated carbon derived from cellulose and cellulose acetate microspheres as electrode materials for symmetric supercapacitors in aqueous electrolytes, Energy Fuels 35 (15) (2021) 12653–12665, https://doi.org/10.1021/acs.energyfuels.1c01449.